JOURNAL OF VIROLOGY, July 2004, p. 6766–6774 Vol. 78, No. 13
0022-538X/04/$08.00+0 DOI: 10.1128/JVI.78.13.6766–6774.2004

Identification of the Human Rhinovirus Serotype 1A Binding Site on the Murine Low-Density Lipoprotein Receptor by Using Human-Mouse Receptor Chimeras

Barbara Herdy, Luc Snyers,† Manuela Reithmayer, Peter Hinterdorfer,‡ and Dieter Blaas*

Max F. Perutz Laboratories, University Departments at the Vienna Biocenter, Department of Medical Biochemistry, University of Vienna, A-1030 Vienna, Austria

Received 7 November 2003/Accepted 22 March 2004

Human rhinovirus serotype 1A (HRV1A) binds more strongly to the mouse low-density lipoprotein receptor (LDLR) than to the human homologue (M. Reithmayer, A. Reischl, L. Snyers, and D. Blaas, J. Virol. 76:6957-6965, 2002). Here, we used this fact to determine the binding site of HRV1A by replacing selected ligand binding modules of the human receptor with the corresponding ligand binding modules of the mouse receptor. The chimeric proteins were expressed in mouse fibroblasts deficient in endogenous LDLR and LDLR-related protein, both used by minor group HRVs for cell entry. Binding was assessed by virus overlay blots, by immunofluorescence microscopy, and by measuring cell attachment of radiolabeled virus. Replacement of ligand binding repeat 5 of the human LDLR with the corresponding mouse sequence resulted in a substantial increase in HRV1A binding, whereas substitution of repeats 3 and 4 was without effect. Replacement of human receptor repeats 1 and 2 with the murine homologues also increased virus binding. Finally, murine receptor modules 1, 2, and 5 simultaneously introduced into the human receptor resulted in HRV1A binding indistinguishable from mouse wild-type receptor. Thus, repeats 1 and/or 2 and repeat 5 are involved in HRV1A attachment. Changing CDGGPD in the acidic cluster of module 5 in the human receptor to CDGEAD present in the mouse receptor led to substantially increased binding of HRV1A, indicating an important role of the glutamate residue in HRV1A recognition.

Human rhinoviruses (HRVs) account for more than 50% of all mild upper respiratory infections known as the common cold. Belonging to the family *Picornaviridae*, they possess an icosahedral capsid composed of 60 copies each of the proteins VP1, 2, 3, and 4 and a single stranded RNA genome with positive polarity roughly 7,100 nucleotides in length. Upon translation, this RNA gives rise to a polyprotein that is cotranslationally and autocatalytically processed to the capsid proteins and to nonstructural polypeptides responsible for viral replication (for a review, see reference 25). Rhinoviruses use unrelated membrane proteins as receptors for cell entry. The 10 minor group HRV serotypes bind the low-density lipoprotein receptor (LDLR), the very low density lipoprotein receptor (VLDLR), and LDLR-related protein (LRP) (9, 13). These membrane receptors are strongly conserved in evolution, and minor group HRVs attach to cells of a number of different species (31). The 91 major group HRVs bind human intercellular adhesion molecule 1 (ICAM-1) (3, 29, 30) and do not attach to the mouse homologue of ICAM-1 (19).

Despite entering mouse cells, wild-type HRV serotype 2 (HRV2), a prototype minor group rhinovirus, fails to replicate in these cells. This indicates that the host restriction is intracellular. A variant of HRV2 that was adapted to grow in mouse L cells showed changes in the nonstructural protein 2C, suggesting that interaction with a specific host factor was involved (37). Similarly, variants of the major group viruses, HRV39 (11) and HRV16 (5), could replicate in mouse L cells when the viral genomic RNA was transfected or human ICAM-1 was stably expressed in the cells to allow for viral attachment. These variants also had changes in 2C. Based on these results, it was believed that wild-type HRVs only replicate in humans and in some primates despite entering cells of other origin. However, our laboratory recently discovered that wild-type HRV1A grows in mouse fibroblasts almost as efficiently as in human cells without requiring adaptation (20). In the course of these studies, we also found that HRV1A preferentially attached to the mouse homologue of LDLR and only weakly bound to human LDLR. Nevertheless, the presence of LRP on human cells is sufficient for effective infection. For these reasons, we decided to use recombinant human-mouse chimeras of LDLR to unravel the basis of this receptor discrimination and to eventually identify the HRV1A attachment site.

A hallmark of all members of the LDLR family is the presence of different numbers of imperfect ligand binding repeats, each about 40 amino acids in length and stabilized by 3 disulfide bonds and a central Ca^{2+} ion (2). LDLR has seven contiguous repeats, and VLDLR has eight contiguous repeats. In LRP, the repeats are arranged in clusters of 2, 8, 10, and 11 modules. Adjacent to the N-terminal ligand binding domains are regions with similarity to epidermal growth factor precursor, a YWTD domain with a β-propeller structure, followed by a more or less O-glycosylated membrane proximal domain, a transmembrane sequence, and a cytoplasmic domain with AP2

* Corresponding author. Mailing address: Max F. Perutz Laboratories, University Departments at the Vienna Biocenter, Department of Medical Biochemistry, University of Vienna, Dr. Bohr Gasse 9/3, A-1030 Vienna, Austria. Phone: 43 1 4277 61630. Fax: 43 1 4277 9616. E-mail: dieter.blaas@meduniwien.ac.at.

† Present address: Institute of Histology and Embryology, University of Vienna, A-1090 Vienna, Austria.

‡ Present address: Institute for Biophysics, J. Kepler University, A-4040 Linz, Austria.

TABLE 1. Primers used in the construction of chimeras and mutants by PCR

Primer	Sequence (5′–3′)[a]
mLDLR.F	TAGTCTCCATTGCACTGGAGGATGAGCACCGCGGATCTGATGC
hLDLR.F	CCATTGTGACTAGTCCATTGC
hLDLR.R	**CAGTCAGTCCAGTACATGAAG**
mLR2.S	**CCCAAGACGTGCTCCCAGG**
hLR2.AS	**TCCTGGGAGCACGTCTTG**
mLR3.S	**TCCTGCCCGGTGA**CCACTTGTGGCCCCGCCCAC
hLR3.AS	GCCACAAGTGGT**CACCGGGCAGGAGGCCTCGTC**
mLR4.S	**CGCTGTAGGGGT**CGAGACACGGCCTCCAAAGGC
hLR4.AS	GGCCGTGTCTCG**ACCCCTACAGCGCTGCGGCCA**
mLR5.AS	**CAGGTGGCC**ACCGCGCAGTGC
hLR5.S	CACTGCGCGGTG**GCCACCTGTCGCCCTGACG**
mLR7.S	ATCAAGGAGTGC**GGGACCAACGAATGC**
hLR7.AS	**TTCGTTGGTCCC**GCACTCCTTGATGGGCTCATC
AF>SL.S	**CTGCTCG**TCCCTG**GAGTTCCACTGCCTA**
AF>SL.AS	**GGAACTC**CAGGGA**CGAGCAGGGGCTACT**
LSG>GSS.S	**CCACTGC**GGT**AGT**AGT**GAGTGCATCCAC**
LSG>GSS.AS	**TGCACTC**ACT**ACT**ACC**GCAGTGGAACTC**
SSWR>RSWV.S	**GCATCCAC**CGC**AGCTGG**GTC**TGTGATGGTGG**
SSWR>RSWV.AS	**CATCACA**GAC**CCAGCT**GCG**GTGGATGCACTC**
GP>EA.S	**GATGGT**GAGGCA**GACTGCAAGGACAAAT**
GP>EA.AS	**TTGCAGTC**TGCCTC**ACCATCACAGCGCC**

[a] Human LDLR sequences are shown in boldface type; mouse sequences are underlined. Sequences identical in both species are shown in boldface type and underlined. hLDLR.F is complementary to the 5′ region flanking the LDLR cDNA in pEFhLDLR806. F, forward; R, reverse; S, sense; AS, antisense. Primers given in the lower section were used for site-directed mutagenesis, e.g., SSWR>RSWV.AS is the reverse primer used to change SSWR to RSWV.

adapter binding motives conferring clathrin-dependent endocytosis (28). Most of these receptors are also involved in signal transduction (17).

A recent investigation has shown that only a single lysine in the HI loop of the viral capsid protein VP1 is strictly conserved within all 10 minor group HRVs. This lysine, together with other basic amino acid residues in the vicinity appears to be responsible for attachment to negatively charged residues in the ligand binding domain of the receptors (34). As determined by cryoelectron microscopy image reconstruction of complexes between recombinant soluble human VLDLR fragments and HRV2 (7), the receptor attaches to these patches of positive surface potential close to the 5 fold axes of the icosahedral viral shell; two consecutive repeats, V2 and V3 of VLDLR, bind two nonequivalent sites present on two neighboring subunits (16). Although the footprint of the receptor on the HRV2 surface was well defined with this technique, its orientation could not be determined due to the small size and the limited resolution of 15 Å.

Whereas the sequences of the ligand binding domain of murine and human VLDLR are very similar (95.1% identity), the two LDLR homologues exhibit only 77% identity (with 226 identical amino acid residues out of 290); these differences must be responsible for their different affinities toward HRV1A. In the present study, we systematically replaced selected ligand binding repeats in the human LDLR with the corresponding ligand binding repeats of the murine homologue and assessed the binding of HRV1A and HRV2 to these chimeric proteins. We demonstrate that LDLR repeat 5 (L5) and L1 and/or L2 provide binding sites for HRV1A. Simultaneous replacement of human L5 (hL5), hL1, and hL2 with the mouse sequences resulted in a protein indistinguishable from the mouse wild-type receptor with respect to HRV1A binding. These data demonstrate the involvement of more than one single repeat in virus binding with a particular role of L5 and L1 and/or L2 in species-specific LDLR attachment of HRV1A.

MATERIALS AND METHODS

Materials. All chemicals were purchased from Sigma (St. Louis, Mo.) unless otherwise specified. Enzymes were from New England Biolabs (Beverly, Mass.). Tissue culture media and supplements were obtained from GibcoBRL (Gaithersburg, Md.). Lipofectamine 2000 was purchased from Invitrogen (Carlsbad, Calif.). Tissue culture plates and flasks were from Costar (Cambridge, Mass.). [^{35}S]methionine/[^{35}S]cysteine was purchased from Hartmann Analytics (Braunschweig, Germany). Benzonase was from Merck (Darmstadt, Germany).

Antibodies. Mouse monoclonal antibodies 8F5 (2.2 mg/ml) against HRV2 (27), 5F9 (hybridoma supernatant) against HRV1A, and chicken immunoglobulin Y (IgY) against the ligand binding domain of LDLR (25 mg/ml) (12) were prepared in the laboratory. Alexa Fluor-conjugated secondary antibodies were obtained from Molecular Probes (Eugene, Oreg.). Cyanine dye-conjugated secondary antibodies and horseradish peroxidase (HRP)-conjugated goat anti-chicken antibodies were obtained from Jackson ImmunoResearch Laboratories (West Grove, Pa.).

Cells and viruses. Simian virus 40 large-T-antigen-immortalized murine fibroblasts (M1) and cells deficient in LRP and LDLR (M4) (6, 10), were kindly provided by Joachim Herz (Southwestern Medical Center, Dallas, Tex.). HRV2 and HRV1A (American Type Culture Collection, Rockville, Md.) were grown and metabolically labeled with ^{35}S in HeLa-H1 cells (Flow Laboratories) as described previously (15). M cells and HeLa cells were cultivated in monolayers in minimal essential medium supplemented with 5 and 10% heat-inactivated fetal calf serum (FCS), respectively, penicillin (100 U/ml), and streptomycin (100 μg/ml).

Construction of LDLR chimeras, site-directed mutagenesis, and expression in M4 cells. All chimeras of the LDLR ligand binding domain were generated by PCR from human (36) and mouse (obtained from Orbigen, San Diego, Calif.) LDLR cDNAs used as templates with the primers listed in Table 1 by following standard protocols. Site-directed mutagenesis (8) was carried out by overlap extension PCR with the primers shown in Table 1 by using a human receptor cDNA, already containing mouse repeat 4, as a template. Receptor DNA was inserted into pEFLDLR806 (20) by using two BstXI restriction sites present in the vector and in the human LDLR cDNA sequence. Note that sequencing of the mouse receptor revealed that V23, G27, K61, P145, K155, A186, and E187 (Swissprot entry) are in fact A23, C27, E61, Q145, N155, G186, and R187, respectively. The latter sequence is identical with that supplied by Orbigen.

LDLR chimeras were stably transfected into M4 cells by using Lipofectamine 2000. After selection in puromycin (2 μg/ml), individual clones were isolated and screened for LDLR expression by immunofluorescence microscopy.

Total cell extracts. Cells (1.2×10^6) stably expressing the LDLR chimeras were seeded in 6-cm-diameter culture dishes and attached during 1 h of incubation at 37°C. After washing with phosphate-buffered saline (PBS), 250 μl of nonreducing Laemmli sample buffer containing 62 U of benzonase was added. Cells were lysed for 1 h at room temperature under agitation. Ten microliters of the lysates was analyzed by sodium dodecyl sulfate (SDS)-polyacrylamide gel electrophoresis.

Western blots. Total cellular proteins were separated under nonreducing conditions on SDS-polyacrylamide gels and electrophoretically transferred to polyvinylidene difluoride membranes (Immobilon-P; Millipore, Bedford, Mass.). The membranes were blocked with PBS containing 2% Tween 20 (blocking buffer) for 1 h and incubated with an IgY preparation from a chicken immunized with recombinant human LDLR, diluted 1:5,000 in PBS–0.1% Tween 20 (incubation buffer), for 1 h. The membranes were washed three times with incubation buffer and incubated for 1 h with HRP-conjugated goat anti-chicken antibody (1:5,000). HRP was detected by using the ECL kit (Pierce, Rockford, Ill.) and Kodak autoradiography films.

Virus overlay blots. HRV2 and HRV1A were metabolically labeled with [^{35}S]methionine/[^{35}S]cysteine (15). Membranes were blocked with Tris-buffered saline containing 2 mM $CaCl_2$ and 2% Tween 20, probed with ~10^4 cpm of ^{35}S-labeled HRV1A or HRV2/ml in 10 ml of Tris-buffered saline containing 2 mM $CaCl_2$ and 0.1% Tween 20 for 1.5 h, and washed three times for 10 min with incubation buffer. The membranes were air dried and autoradiographed for 24 h with Kodak MR films.

Fluorescence microscopy. Cells were grown on coverslips until 70% confluent and infected with HRV2 or HRV1A at 35 PFU/cell in minimal essential medium supplemented with 2% FCS, 30 mM $MgCl_2$, 2 mM L-glutamine, and antibiotics (infection medium) for 20 min at 34°C. They were washed once with PBS, fixed in 3% paraformaldehyde in PBS for 15 min at room temperature, and quenched for 10 min in 50 mM NH_4Cl in PBS. After washing with PBS, cells were permeabilized with 0.1% Triton X-100 in PBS for 5 min, washed again with PBS, and blocked in 5% FCS in PBS for 10 min. Incubation with monoclonal antibody 8F5 (against HRV2, diluted 1:250 in PBS containing 1% FCS) or monoclonal antibody 5F9 (against HRV1A, hybridoma supernatant) was performed for 45 min at room temperature. For simultaneous detection of LDLR expression, IgY anti-LDLR (diluted 1:1,000 in PBS containing 1% FCS) was used. Cells were washed with PBS and incubated with goat anti-mouse Alexa 488 (1:1,000) and goat anti-chicken Cy3 fluorophore-conjugated (1:250) secondary antibodies for 1 h at room temperature. The coverslips were washed three times with PBS, rinsed briefly in double-distilled H_2O, and mounted in Vectashield mounting medium (Vector Laboratories, Burlingame, Calif.). Samples were viewed under a Leica TCS NT confocal microscope (Heidelberg, Germany). Images were processed by using Adobe Photoshop software with the same parameters for all images.

Quantification of receptor expression and of virus binding and internalization. Cells grown in 24-well plates until ~80% confluence were washed twice with PBS, fixed with 3% paraformaldehyde in PBS for 40 min at room temperature, and quenched for 10 min in 50 mM NH_4Cl. After washing with PBS, the cells were blocked with 2% bovine serum albumin (BSA) in PBS for 1 h, incubated with anti-LDLR IgY (1:1,000) in PBS containing 0.1% BSA for 1 h, washed three times with 0.1% BSA in PBS, and incubated with HRP-conjugated anti-chicken antibody (1:5,000) for 1 h. After washing four times with PBS, HRP was revealed with 300 μl of 3,3′,5,5′-tetramethyl benzidine (100 μg/ml) and 0.03% H_2O_2 in 100 mM Na acetate (pH 5.6) for 10 min. The reaction was halted with 1/2 volume of 1 M H_2SO_4, and absorbance was determined on a microplate reader at 450 nm. For determination of virus binding, about 10,000 cpm of [^{35}S]methionine-labeled HRVs (15) in 200 μl of infection medium was added to subconfluent cells grown in 24-well plates. After incubation for 30 min at 34°C, the cells were washed with PBS, and radioactivity in the supernatants plus wash and in the cells recovered by trypsinization was determined by liquid scintillation counting as described previously (20).

Model building. L5 sequences from the species indicated were submitted to automatic modeling with SwissModel (4, 18, 24). The models obtained were superimposed onto the known structure of hL5 by using Magic Fit in Swiss-PdbViewer, version 3.7, and the surface potentials were calculated and visualized with colors set to −5.0 (red), −3.0 (white), and +1.0 (blue). The superimposed models were arranged identically as to turn the face with the strongest negative charge in hL5 towards the viewer; the models are centered on the tryptophan that, in V3, has been shown to be directly involved in interaction with the aliphatic side chain of the conserved lysine in the BC loop of HRV2 (33). The validity of the approach was tested by modeling hL5 based on nuclear magnetic resonance (NMR) structures of hL6 (1f8zA.pdb and 1d2jA.pdb) and of LRP CR8 (1cr8A.pdb) but omitting the X-ray structures of hL5 (1n7dA.pdb and 1ajj_.pdb).

RESULTS

HRV1A and HRV2 bind with different efficiencies to chimeric human and mouse LDLR in virus overlay blots. HRV1A binds well to mouse LDLR but only very weakly attaches to the human receptor homologue. To identify the receptor module(s) responsible, ligand binding repeats of the human receptor were systematically replaced by the corresponding mouse modules and binding of the two virus serotypes to these chimeric proteins was assessed. The plasmid pEFLDLR806 (28), encoding human LDLR that lacks 33 amino acids including the coated pit targeting signal at its C terminus, was used as a starting point for the construction of human-mouse LDLR chimeras. Upon stable transfection into mouse M4 cells that are deficient in LDLR and LRP expression as a consequence of gene disruption (10, 35), the truncated receptor was produced at a 25- to 50-fold-higher level than the full-length receptor (28). This is most probably due to reduced internalization and lysosomal degradation. Human-mouse LDLR chimeras, as summarized in Fig. 1, were then constructed and stably transfected into M4 cells. One clone was selected from each construct based on high expression level. The amounts of the recombinant LDLR chimeras present in the cells were compared on Western blots by using antibodies recognizing both human and mouse LDLR (14). As seen in the Western blots in Fig. 2A, the expression levels of the human receptor, the chimera carrying the entire binding domain of the murine receptor (m1-7), and the various other chimeric receptors were similar but not identical; this was confirmed by using an enzyme-linked immunosorbent assay (ELISA)-type assay (Table 2). As expected, for nontransfected M4 cells, no LDLR was seen in the Western blot (Fig. 2A) and the ELISA revealed only background binding (Table 2). Sometimes a second and a third band migrating in front of the main band were observed at various intensities; these polypeptides presumably correspond to misfolded, inactive forms of the recombinant proteins, since they did not bind the HRVs in virus overlay blots (Fig. 2). HRV2 (Fig. 2B) bound to all receptor variants. In accord with earlier results (20), attachment of HRV1A to the human receptor was not detectable (Fig. 2C). Binding to m3-4 and to m4 was also below the detection limit. However, HRV1A bound to all constructs containing m5 alone or m5 together with other mouse repeats. In a separate experiment, HRV binding to chimeras containing mouse repeats m1 and m2 was also assessed (right panels). HRV2 as well as HRV1A bound to m1-7, m1-2, and m1-2 and m5. These results suggest that m5 as well as m1 and/or m2 are involved in HRV1A binding. This was confirmed by a more quantitative assay (see below, Table 2, and Fig. 6).

To support these in vitro data and to exclude possible effects of denaturation during the separation of the receptors on the polyacrylamide-SDS gels and Western blotting, binding of the two virus serotypes to cells expressing the various chimeras was assessed by indirect immunofluorescence microscopy. Cells grown on coverslips were incubated with HRV2 or HRV1A for

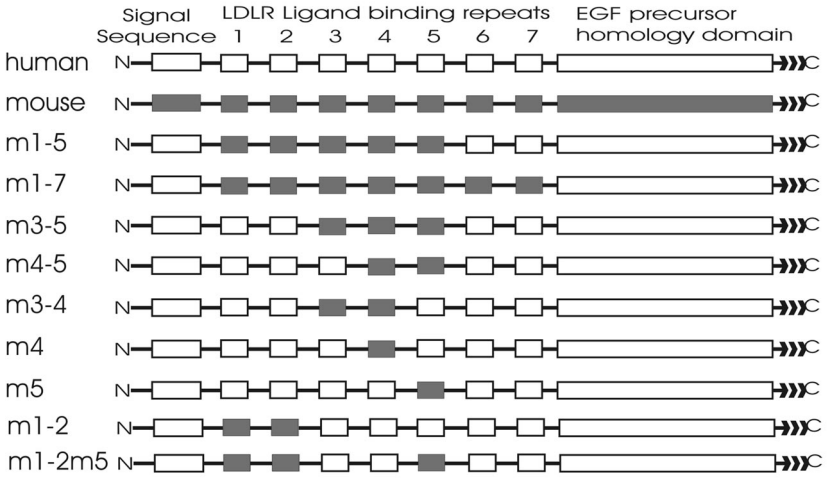

FIG. 1. Scheme of the chimeric LDLR used. In human LDLR, carrying a deletion of part of the C-terminal cytoplasmic domain including the clathrin localization signal, ligand binding repeats (white boxes) were exchanged for the corresponding murine repeats (gray boxes) and the cDNA plasmids were stably transfected into receptor-negative mouse M4 cells. The scheme is not drawn to scale, and the transmembrane region and cytoplasmic tail are indicated by triple angle brackets. EGF, epidermal growth factor.

20 min at 34°C to allow for virus binding and internalization (28). The cells were fixed and stained with anti-LDLR antibodies, verifying the expression of the chimeric proteins (Fig. 3, upper and lower panels). HRV binding was assessed with monoclonal antibodies specific for the respective viral serotypes followed by Alexa 488-labeled secondary antibodies. HRV2 bound similarly to all chimeras (Fig. 3), whereas HRV1A bound well to all receptor constructs except those containing murine repeats 3-4 or 4; likewise, it did not bind to the human receptor. This, again, strongly suggests a predominant role of repeat 5 and repeats 1 and/or 2 in the interaction between HRV1A and LDLR.

Amino acid residues involved in virus binding. Since murine repeat 5 alone in the context of the human receptor was able to confer HRV1A binding, we decided to analyze this repeat in more detail. Sequence comparison of L5 from mice and humans reveals that, of the 39 amino acid residues (Swissprot annotation), 30 are identical (Fig. 4). These include the four most conserved aspartic and glutamic acids involved in chelating the central Ca^{2+} ion (2) and the six cysteines. To further cut down the number of amino acid residues potentially responsible for receptor discrimination, we compared various species whose LDLR sequences are known, with respect to discriminative binding. Lysates from HeLa cells, mouse fibroblasts (M1), rat embryo fibroblasts (REF), Chinese hamster ovary cells (CHO), and rabbit kidney cells (RK13) were analyzed in parallel by virus overlay blotting with radiolabeled HRV2 and HRV1A (data not shown). Whereas all LDLR homologues bound HRV2 to a similar extent, HRV1A showed strong binding to the mouse and to the rabbit protein only, and it did not bind to human protein and only weakly bound to rat and hamster LDLR (Fig. 4). The difference in HRV1A binding

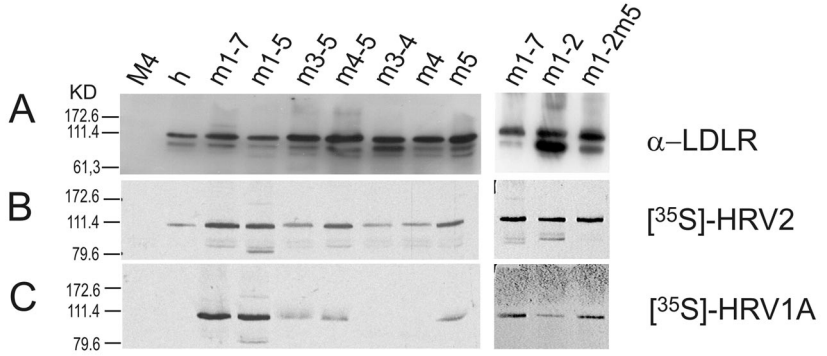

FIG. 2. Cell extracts from the same number of cells expressing the various human-mouse LDLR chimeras lacking the clathrin localization signal (Fig. 1) were prepared and separated in parallel on 10% polyacrylamide–SDS gels under nonreducing conditions. Proteins were electrotransferred to polyvinylidene difluoride membranes, and LDLR was revealed with anti-LDLR (α-LDLR) IgY (A), ~100,000 cpm of ^{35}S-labeled HRV2 (B), and ~100,000 cpm of ^{35}S-labeled HRV1A (C). IgY was revealed with secondary HRP-conjugated rabbit anti-IgY antibody and chemiluminescent substrate; radioactivity was directly revealed on X-ray film. M4, nontransfected M4 cells used as receptor-negative control; h, M4 cells expressing human LDLR; m, M4 cells expressing human LDLR in which the repeats indicated were exchanged for the murine homologues. The relative molecular masses of marker proteins run on the same gels are indicated. Note that the panels on the right are from a different experiment; m1-7 was also included to allow for comparison with the panel on the left.

TABLE 2. LDLR expression of and HRV binding to cell lines stably transfected with human-mouse LDLR chimeras[c]

Cell line	LDLR expression[a]	% of virus bound[b]		HRV1A/HRV2 ratio
		HRV2	HRV1A	
M4	0.23 ± 0.032	2.9 ± 0.85	5.6 ± 1.82	1.930
M4-h	0.85 ± 0.075	34.6 ± 3.08	8.9 ± 4.38	0.258
M4-m1-7	0.61 ± 0.026	23.2 ± 3.73	27.6 ± 5.84	1.191
M4-m1-5	0.61 ± 0.082	30.4 ± 6.82	36.3 ± 4.69	1.195
M4-m3-5	0.97 ± 0.059	22.1 ± 2.85	25.5 ± 6.13	1.150
M4-m4-5	0.99 ± 0.003	23.6 ± 4.54	28.3 ± 10.47	1.197
M4-m3-4	0.93 ± 0.039	44.8 ± 10.39	5.7 ± 1.98	0.127
M4-m4	0.76 ± 0.044	23.2 ± 4.88	6.9 ± 3.58	0.298
M4-m5	0.75 ± 0.034	15.1 ± 2.68	9.1 ± 1.16	0.603
M4-m1-2	0.51 ± 0.027	14.4 ± 3.20	10.1 ± 2.23	0.701
M4-m1-2m5	0.48 ± 0.040	21.8 ± 7.23	30.0 ± 2.54	1.376
AF>SL	0.68 ± 0.055	19.1 ± 3.31	6.5 ± 2.73	0.339
LSG>GSS	1.08 ± 0.047	52.3 ± 11.11	7.1 ± 4.48	0.135
SSWR>RSWV	0.96 ± 0.045	31.8 ± 4.91	6.0 ± 2.48	0.190
GP>EA	0.67 ± 0.066	16.2 ± 4.76	23.8 ± 6.82	1.475

[a] LDLR expressed on the cell surface was determined by ELISA. The A_{450} of the HRP substrate was determined on a microplate reader.
[b] ^{35}S-labeled HRVs were incubated with the cells, and bound radioactivity is given as the percentage of total radioactivity present in the assay.
[c] Results for LDLR expression and virus binding are means of the results from 3 to 5 independent experiments ± standard deviations.

between rat and mouse LDLR was unexpected, since only 2 residues in L5 are not identical. It is thus likely that these residues are directly involved in virus binding.

Based on the strong basic surface potential of the receptor binding site in all minor group HRVs (34) and the known involvement of negative charges of the LDLR in ligand recognition (1), we assumed that a negative surface potential is also responsible for HRV recognition. This led us to suggest that Glu199 in the mouse protein (Fig. 4) was involved in the interaction with HRV1A, as it is replaced by uncharged residues in the weakly binding human, rat, and hamster homologues. Furthermore, it is the only residue different between mouse and rat L5 within the negative charge cluster surrounding the central Ca^{2+} ion.

Site-directed mutagenesis of hL5. To assess whether Glu199 in mouse L5 was indeed required for binding of HRV1A and to verify that no other residues were involved, selected amino acid pairs in hL5 were exchanged for those present in the mouse (Fig. 4). M4 cells were stably transfected with the plasmids encoding human LDLR with L5 carrying the mutations indicated in Fig. 4. Clones showing high-level expression of the foreign protein, as judged by HRV2 binding by immunofluorescence microscopy, were selected. Discriminative virus binding was then assessed by immunofluorescence as in Fig. 3.

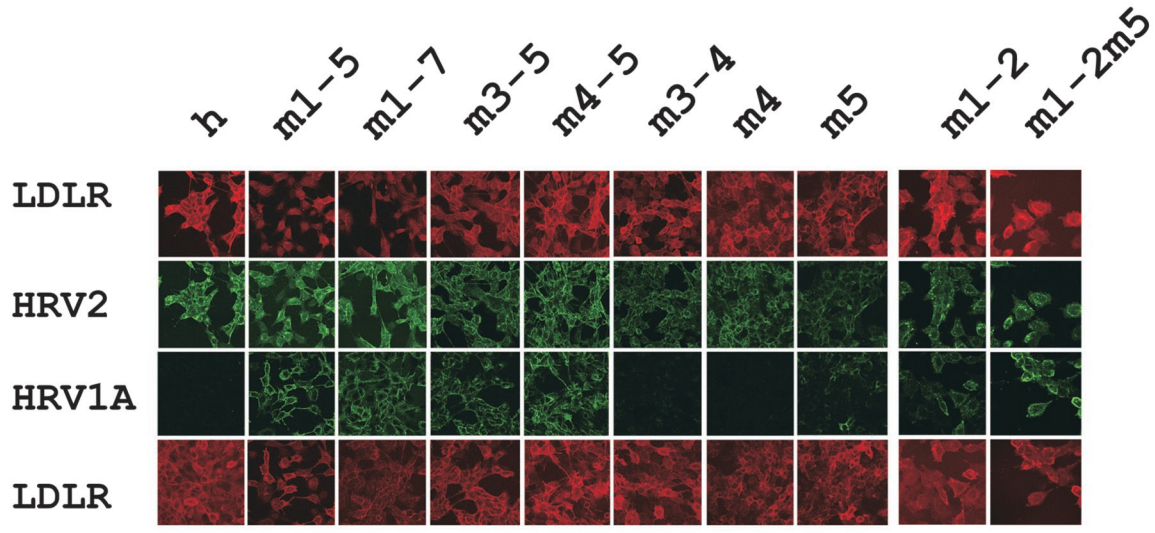

FIG. 3. Virus binding assessed by indirect immunofluorescence microscopy of M4 cells stably transfected with the human-mouse chimeric LDLR as indicated. Cells grown on coverslips were incubated with 10^8 $TCID_{50}$/ml (MOI, ~35) of the respective HRV serotypes for 20 min at 34°C, washed, and fixed, and eventually bound virus was detected with monoclonal antibody 8F5 (HRV2) or 5F9 (HRV1A) followed by Alexa 488-conjugated secondary antibody. Receptor expression was monitored with IgY directed against LDLR followed by Cy3-conjugated anti-chicken IgY antibody. Cells were viewed under a confocal fluorescence microscope, and all samples were photographed with the same parameter settings. Note that the two panels on the right (m1-2 and m1-2m5) are from a different experiment.

```
                                                                  BINDING OF
                                  LDL-RECEPTOR REPEAT 5           HRV1A HRV2
mutant #                        1      2      3     4
L5 human(P01130)  174SPCSAFEFHCLSGECIHSSWRCDGGPDCKDKSDEENCAV212-   +
L5 mouse(P35951)  175SPCSSLEFHCGSSECIHRSWVCDGEADCKDKSDEEHCAV213+   +
L5 rat(P35952)      SPCSSLEFHCGSSECIHRSWVCDGAADCKDKSDEENCAV  -   +
L5 rabbit(P20063)   GPCSRHEFHCGSGECVHASWRCDGDADCRDGSDERDCAA  +   +
L5 hamster(P35950)  SPCSSLEFHCGSSECIHRSWVCDGSADCKDKSDEEHCVT  -   +
consensus            PCS  EFHC S EC H SW CDG ADCKD SDE  C
V3 human (P98155)RTCRIHEISCGAHSTQCIPVSWRCDGENDCDSGEDEENCGN  +   +
                                  !   ^  !  ^      ^^
```

FIG. 4. Alignment of the amino acid sequences of LDLR repeat 5 from various species and of human VLDLR repeat 3. The Swissprot entry codes are indicated for each sequence. Residues of the human repeat whose coordinates are available from X-ray crystallography (2) are underlined. Carets on the bottom of the figure point to those residues whose side chains coordinate with Ca^{2+}; exclamation points point to the two residues whose main-chain oxygens participate in Ca^{2+} coordination. L5 residues identical in all shown species are indicated as consensus. +, strong binding; −, weak binding. The only two amino acid residues different between the mouse and rat are depicted in italics in the rat sequence. Residue pairs in hL5, which were replaced by site-directed mutagenesis for those present in the mouse sequence, are depicted in boldface type in gray blocks and are numbered consecutively. The glutamate important in HRV1A binding is underlined. Note that numbering is from the first amino acid after the signal peptide cleavage site. The precursor protein thus contains 21 additional residues at its N terminus.

Except for the exchange of GlyPro198-199 for GluAla (GP→EA), all mutations were without effect on HRV1A binding (Fig. 5). Only the latter mutation resulted in substantially increased HRV1A binding. These results underscore the importance of the glutamic acid residue at this position for the recognition of HRV1A. Since the alanine next to the glutamic acid residue is also present at the equivalent position in the rat receptor, which only binds weakly, we believe that this residue is not important. Nevertheless, in the absence of additional mutational data, we cannot exclude that Pro200 also contributes by modifying the conformation of Glu199. This result again strongly supports the contention that the acidic cluster is involved in direct interaction with the virus. We thus believe that this face of the molecule contacts the HI and the BC loop of VP1 when complexed to the viral capsid.

Quantification of receptor expression and virus binding. The validity of the attachment tests employed was further verified by using more quantitative assays. All cell clones expressing the various receptor chimeras and mutants were grown in parallel in 24-well plates, and surface expression of the receptors was determined by an ELISA. As seen in Table 2, all receptors were expressed but not to identical levels. This is not unexpected, since integration of the receptor cDNA into the genome occurs largely at random, and positional effects govern the expression level. The cells were then challenged with radiolabeled HRV1A and HRV2, respectively, and incu-

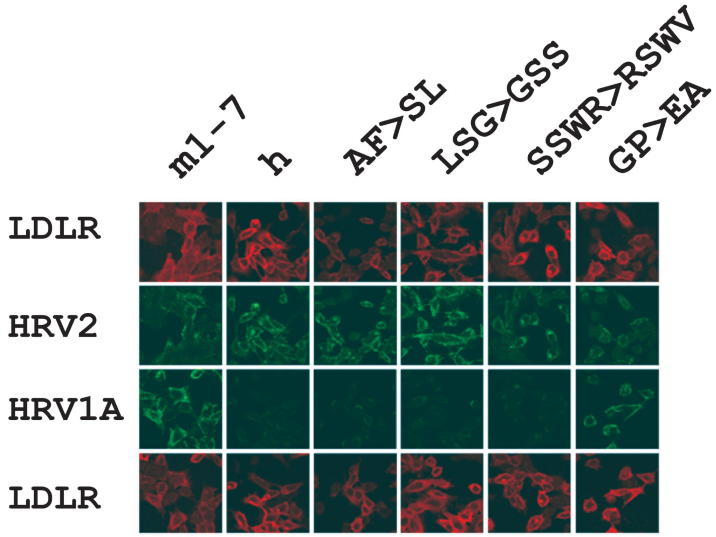

FIG. 5. Virus binding assessed by indirect immunofluorescence microscopy of M4 cells stably transfected with human LDLR carrying the mutations indicated. Cells grown on coverslips were incubated with 10^8 $TCID_{50}$/ml (MOI, ~35) of the respective HRV serotypes for 20 min at 34°C, washed, and fixed, and eventually bound virus was detected with monoclonal antibody 8F5 (HRV2) or 5F9 (HRV1A) followed by Alexa 488-conjugated secondary antibody. Receptor expression was monitored with IgY directed against LDLR followed by Cy3-conjugated anti-chicken IgY antibody. Cells were viewed under a confocal fluorescence microscope, and all samples were photographed with the same parameter settings. Receptors carrying the entire mouse (m1-7) and human (h) ligand binding domains were included as controls.

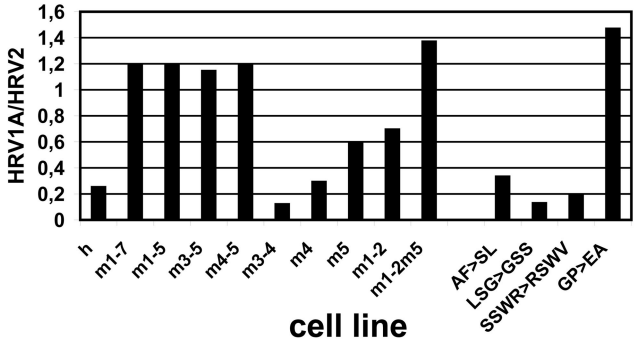

FIG. 6. Ratio between HRV1A and HRV2 binding and internalization. M4 cells expressing the various chimeric receptors were grown in 24-well plates and challenged with about 10,000 cpm of radiolabeled HRV1A and HRV2, respectively, for 30 min at 34°C and washed, and cell-associated radioactivity divided by total radioactivity in the assay was determined by liquid scintillation counting. Data are from Table 2.

bated for 30 min at 34°C. Although the receptor constructs lack a functional internalization signal (28), their high expression rates result in some virus also being internalized. Thus, our assay measures binding plus internalization. Even when taking into account differences in receptor expression, the association of HRV2 to the different constructs was not equal (Table 2). Reasons for this might be differences in folding, transport, and/or internalization. However, since the variation in receptor expression and the effects mentioned above will affect both serotypes to the same extent, they are of no concern for the analysis of relative binding of HRV1A and HRV2 (Table 2 and Fig. 6). The results of these experiments extend the data presented in Fig. 2, 3, and 5 in that the presence of m1-2 or m5 in the background of human LDLR increases HRV1A binding. HRV1A bound to all constructs containing m5 plus additional mouse repeats to a similar extent as HRV2. Finally, quantification of the binding to the mutant receptors (Fig. 6, right panel) again underscores the importance of the glutamic acid residue (compare to Fig. 4 and 5) within L5 in binding of this particular serotype.

DISCUSSION

LDLR is strongly conserved throughout evolution, and the cysteines forming disulfide bonds together with the residues complexed with the Ca^{2+} ion are at identical positions in most of the ligand binding repeats. Nevertheless, HRV1A was found to bind more strongly to the mouse homologue than to the human version of the receptor (20). To assess whether a particular repeat was responsible for this specificity, we systematically replaced human repeats for mouse repeats (Fig. 1) and expressed the chimeric receptors in a mouse cell line deficient in LDLR and LRP expression. This avoids problems with misfolding that might occur in in vitro binding assays employing bacterially expressed proteins (21). Virus overlay blots from cell extracts (Fig. 2) and immunofluorescence microscopy (Fig. 3) demonstrated that the presence of murine L5 in the context of the human receptor was sufficient for HRV1A binding. The exchange of repeats 1 and 2 with the corresponding murine repeats had a similar effect, and the presence of all of these three murine repeats (m1, m2, and m5) resulted in HRV1A attachment almost identical to that of the entire mouse receptor. This was confirmed by measuring the cell binding of radiolabeled HRVs (Table 2 and Fig. 6). The results are similar to findings by Esser and colleagues (1), who have shown by deletion analysis that L5 was essential for binding of β-VLDL but that other repeats also contributed. The increase in binding upon replacement of hL1 and hL2 for mouse L1 and L2 is in line with the possible involvement of L2 in LDL binding. A variant of LDLR lacking the first two repeats leads to familial hypercholesterolemia (23), but L1 is dispensable for lipoprotein binding (32).

Concentrating on L5, we then analyzed the LDLR of several species for discrimination between HRV1A and HRV2 and found that, in addition to the mouse receptor, the rabbit receptor bound HRV1A strongly, whereas like the human receptor, the rat and hamster receptors displayed only marginal binding. This is particularly interesting, since mouse and rat L5 share all but two residues (Fig. 4). Based on these data, we exchanged selected amino acid residues in L5 of the human receptor (containing mouse L4) for those present in the mouse and found that the change (in italics) from CDG*GP*D to CDG*EA*D in the acidic cluster conferred HRV1A binding activity to the human receptor. Since the alanine is also present in the rat, we believe that the exchange of glycine to glutamate is sufficient to acquire specific binding of HRV1A. All of these findings were confirmed by a more quantitative binding assay with radiolabeled HRVs (Fig. 6).

Based on alignments of L4 and L5 with V5 and V6 (repeats 5 and 6 of VLDLR) of various species and by using the X-ray structure of the entire LDLR at low pH, it was proposed (22) that these repeats interact with the β-propeller in the low-pH environment present in endosomal compartments. This latter structure is believed to intramolecularly compete for the binding site with the ligands, resulting in their dissociation from LDLR. According to this model, among other residues, W193, D196, and D200 in L5 (numbering from the first amino acid in the mature protein) establish contacts with E581 and K582 of the β-propeller. W193 is exposed to solvent and interacts with the aliphatic part of the side chains while the acidic groups create a strong negative-charge cluster, establishing interactions with the ε-amino group of the lysine. On these grounds, we believe that the lysine (K224 in VP1 of HRV2), which is conserved in all minor group HRVs, interacts with W193, D196, and D200. Indeed, the recently solved X-ray structure of a complex between HRV2 and V23, a tandem of repeats 2 and 3 of VLDLR (33), shows contacts of the aliphatic side chain of K224 with the tryptophan and of its ε-amino group with the glutamic acid of V3 (compare to Fig. 4). Since the aspartates contribute with their carboxylates to the Ca^{2+} complex, they are not available for ionic interactions but nevertheless provide a negative electrostatic potential (Fig. 7). Glycine 198 in L5 contributes with its amide oxygen to Ca^{2+} chelation (2); a glutamic acid at its position might thus have its carboxylate free to make a salt bridge with the lysine in the HI loop of VP1 on the viral surface.

Comparisons of repeat L5 with repeats CR3, CR7, and CR8 from LRP indicated a very similar overall conformation despite substantial sequence diversity (26). Therefore, we believe that automatic modeling of the three-dimensional structure of repeats with so far unknown structure based on the available

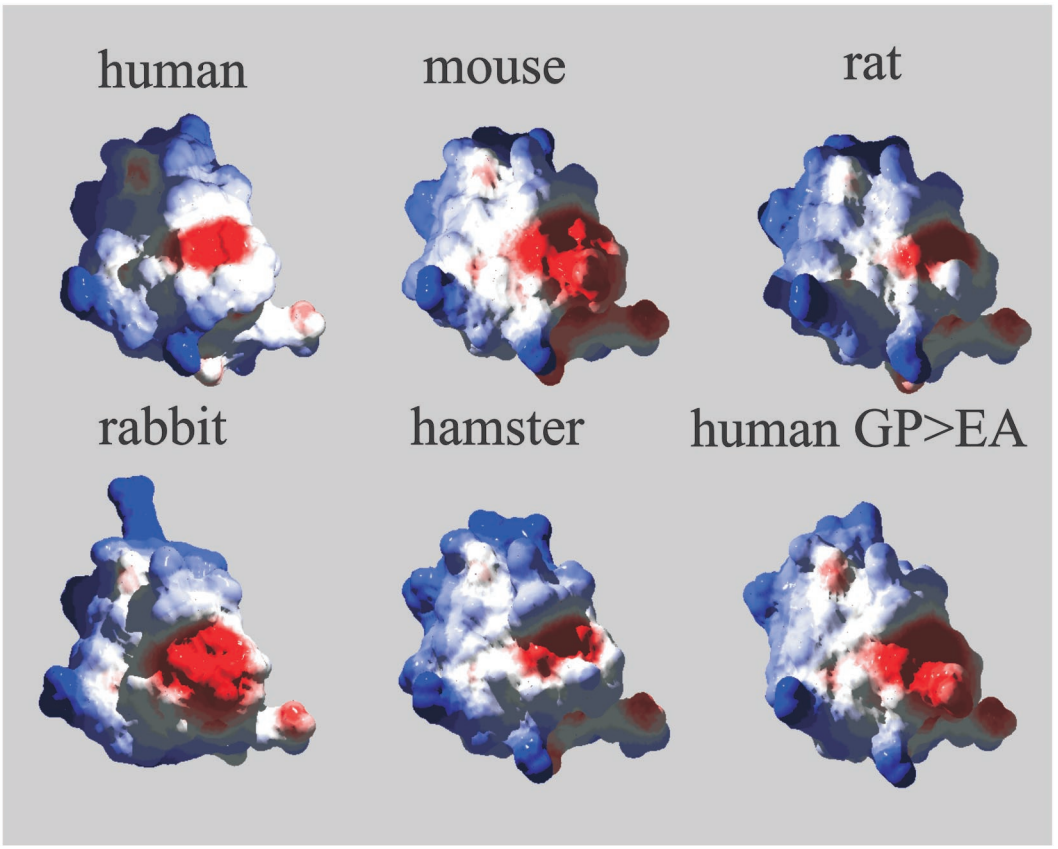

FIG. 7. Comparison of the surface potentials of repeat 5 from various species. The sequences of repeat 5 of the murine, rat, rabbit, hamster, and hL5 sequences carrying the GlyPro→GluAla mutation were submitted to SwissModel for structure prediction based on the known coordinates of all LDLR modules present in the database. Surface potentials were color coded (−5.0, red; −3.0, white; +1.0, blue) by using SpdbViewer and arranged as to turn the face with the strongest negative charge towards the viewer. The view is centered on W193, with the N terminus on the left and the C terminus on the right. The figure was rendered with POV-Ray 3.5. Note that all but the structure of hL5 are models calculated with SwissModel.

X-ray and NMR coordinates of related repeats (2, 22) might be rather accurate. First, we assessed the adequacy of the approach by building a model of hL5 with SwissModel (4, 18, 24) by using the NMR structures of hL6 and human LRP CR8 as templates but omitting the two available X-ray structures of hL5 present in the data bank (no other structures were selected as templates by automatic modeling). Despite the sequence identity between hL5 and hL6 and CR8 being only 48 and 64%, respectively, the root mean square deviation between the X-ray structure and the model obtained (including side chains) was 1.24 Å. Considering the much higher identities between hL5 and its homologues (between 70% for rabbit and 79% for rat), models built by inclusion of the two X-ray structures of hL5 are certainly of much higher quality. We thus calculated three-dimensional models of L5 of the different species, previously tested for virus binding (Fig. 4), and examined their surface potentials for the presence of prominent charge patterns (Fig. 7). The electrostatic potential map indicates, as expected, that Glu199 in the mouse substantially increases the negative surface potential in the CDXEXDC sequence (with the 2 D's contributing their carboxylates to Ca^{2+} chelation) compared to the human homologue. This is similar for the rabbit sequence CDGDADC, containing an aspartate at the same position and for the mutant human protein in which GlyPro was exchanged for GluAla (Fig. 4). The absence of an acidic residue at the equivalent position in the rat and hamster leads to a reduction in the overall negative potential.

Determination of the structure of a complex between HRV2 and various recombinant VLDLR fragments by cryoelectron microscopy revealed that V3 was bound to the HI and BC loops in VP1; however, V2 was also bound, although weakly, to a nonequivalent site on the HI loop of the neighboring subunit (7, 16). Therefore, it is likely that two or even more repeats unequally contribute to the overall binding strength. As indicated by the stronger binding of chimeras containing more than two mouse repeats, in particular m1 and m2 plus m5, repeats other than L5 are able to attach. As L1 has been shown to be dispensable for binding LDL and VLDL (32), most probably only L2 is involved. As shown here for HRV1A, single amino acid differences in the modules have a strong influence on receptor attachment and might result in a loss of binding. Nevertheless, infection is still possible because the virus always finds a suitable binding partner in the large selection of receptor modules present within the members of the LDLR family.

ACKNOWLEDGMENTS

This work was funded by the Austrian Science Foundation grant P-14503 to D.B. and P14549 to P.H.

We thank Irene Goesler for preparation of virus and monoclonal antibody 5F9.

REFERENCES

1. **Esser, V., L. E. Limbird, M. S. Brown, J. L. Goldstein, and D. W. Russell.** 1988. Mutational analysis of the ligand binding domain of the low density lipoprotein receptor. J. Biol. Chem. **263:**13282–13290.
2. **Fass, D., S. Blacklow, P. S. Kim, and J. M. Berger.** 1997. Molecular basis of familial hypercholesterolaemia from structure of LDL receptor module. Nature **388:**691–693.
3. **Greve, J. M., G. Davis, A. M. Meyer, C. P. Forte, S. C. Yost, C. W. Marlor, M. E. Kamarck, and A. McClelland.** 1989. The major human rhinovirus receptor is ICAM-1. Cell **56:**839–847.
4. **Guex, N., and M. C. Peitsch.** 1997. SWISS-MODEL and the Swiss-Pdb-Viewer: an environment for comparative protein modeling. Electrophoresis **18:**2714–2723.
5. **Harris, J. R., and V. R. Racaniello.** 2003. Changes in rhinovirus protein 2C allow efficient replication in mouse cells. J. Virol. **77:**4773–4780.
6. **Herz, J., D. E. Clouthier, and R. E. Hammer.** 1992. LDL receptor-related protein internalizes and degrades uPA-PAI-1 complexes and is essential for embryo implantation. Cell **71:**411–421.
7. **Hewat, E. A., E. Neumann, J. F. Conway, R. Moser, B. Ronacher, T. C. Marlovits, and D. Blaas.** 2000. The cellular receptor to human rhinovirus 2 binds around the 5-fold axis and not in the canyon: a structural view. EMBO J. **19:**6317–6325.
8. **Ho, S. N., H. D. Hunt, R. M. Horton, J. K. Pullen, and L. R. Pease.** 1989. Site-directed mutagenesis by overlap extension using the polymerase chain reaction. Gene **77:**51–59.
9. **Hofer, F., M. Gruenberger, H. Kowalski, H. Machat, M. Huettinger, E. Kuechler, and D. Blaas.** 1994. Members of the low density lipoprotein receptor family mediate cell entry of a minor-group common cold virus. Proc. Natl. Acad. Sci. USA **91:**1839–1842.
10. **Ishibashi, S., M. S. Brown, J. L. Goldstein, R. D. Gerard, R. E. Hammer, and J. Herz.** 1993. Hypercholesterolemia in low density lipoprotein receptor knockout mice and its reversal by adenovirus-mediated gene delivery. J. Clin. Investig. **92:**883–893.
11. **Lomax, N. B., and F. H. Yin.** 1989. Evidence for the role of the P2 protein of human rhinovirus in its host range change. J. Virol. **63:**2396–2399.
12. **Marlovits, T. C., C. Abrahamsberg, and D. Blaas.** 1998. Soluble LDL mini-receptors. Minimal structure requirements for recognition of minor group human rhinovirus. J. Biol. Chem. **273:**33835–33840.
13. **Marlovits, T. C., C. Abrahamsberg, and D. Blaas.** 1998. Very-low-density lipoprotein receptor fragment shed from HeLa cells inhibits human rhinovirus infection. J. Virol. **72:**10246–10250.
14. **Marlovits, T. C., T. Zechmeister, M. Gruenberger, B. Ronacher, H. Schwihla, and D. Blaas.** 1998. Recombinant soluble low density lipoprotein receptor fragment inhibits minor group rhinovirus infection in vitro. FASEB J. **12:**695–703.
15. **Neubauer, C., L. Frasel, E. Kuechler, and D. Blaas.** 1987. Mechanism of entry of human rhinovirus 2 into HeLa cells. Virology **158:**255–258.
16. **Neumann, E., R. Moser, L. Snyers, D. Blaas, and E. A. Hewat.** 2003. A cellular receptor of human rhinovirus type 2, the very-low-density lipoprotein receptor, binds to two neighboring proteins of the viral capsid. J. Virol. **77:**8504–8511.
17. **Nykjaer, A., and T. E. Willnow.** 2002. The low-density lipoprotein receptor gene family: a cellular Swiss army knife? Trends Cell Biol. **12:**273–280.
18. **Peitsch, M. C.** 1995. Protein modelling by e-mail. Bio/Technology **13:**658–660.
19. **Register, R. B., C. R. Uncapher, A. M. Naylor, D. W. Lineberger, and R. J. Colonno.** 1991. Human-murine chimeras of ICAM-1 identify amino acid residues critical for rhinovirus and antibody binding. J. Virol. **65:**6589–6596.
20. **Reithmayer, M., A. Reischl, L. Snyers, and D. Blaas.** 2002. Species-specific receptor recognition by a minor-group human rhinovirus (HRV): HRV serotype 1A distinguishes between the murine and the human low-density lipoprotein receptor. J. Virol. **76:**6957–6965.
21. **Ronacher, B., T. C. Marlovits, R. Moser, and D. Blaas.** 2000. Expression and folding of human very-low-density lipoprotein receptor fragments: neutralization capacity toward human rhinovirus HRV2. Virology **278:**541–550.
22. **Rudenko, G., L. Henry, K. Henderson, K. Ichtchenko, M. S. Brown, J. L. Goldstein, and J. Deisenhofer.** 2002. Structure of the LDL receptor extracellular domain at endosomal pH. Science **298:**2353–2358.
23. **Sass, C., L. M. Giroux, S. Lussiercacan, J. Davignon, and A. Minnich.** 1995. Unexpected consequences of deletion of the first two repeats of the ligand-binding domain from the low density lipoprotein receptor. Evidence from a human mutation. J. Biol. Chem. **270:**25166–25171.
24. **Schwede, T., J. Kopp, N. Guex, and M. C. Peitsch.** 2003. SWISS-MODEL: an automated protein homology-modeling server. Nucleic Acids Res. **31:**3381–3385.
25. **Semler, B. L., and E. Wimmer.** 2002. Molecular biology of picornaviruses. ASM Press, Washington, D.C.
26. **Simonovic, M., K. Dolmer, W. Huang, D. K. Strickland, K. Volz, and P. G. Gettins.** 2001. Calcium coordination and pH dependence of the calcium affinity of ligand-binding repeat CR7 from the LRP. Comparison with related domains from the LRP and the LDL receptor. Biochemistry **40:**15127–15134.
27. **Skern, T., C. Neubauer, L. Frasel, P. Gruendler, W. Sommergruber, W. Zorn, E. Kuechler, and D. Blaas.** 1987. A neutralizing epitope on human rhinovirus type 2 includes amino acid residues between 153 and 164 of virus capsid protein VP2. J. Gen. Virol. **68:**315–323.
28. **Snyers, L., H. Zwickl, and D. Blaas.** 2003. Human rhinovirus type 2 is internalized by clathrin-mediated endocytosis. J. Virol. **77:**5360–5369.
29. **Staunton, D. E., V. J. Merluzzi, R. Rothlein, R. Barton, S. D. Marlin, and T. A. Springer.** 1989. A cell adhesion molecule, ICAM-1, is the major surface receptor for rhinoviruses. Cell **56:**849–853.
30. **Tomassini, E., T. Graham, C. DeWitt, D. Lineberger, J. Rodkey, and R. Colonno.** 1989. cDNA cloning reveals that the major group rhinovirus receptor on HeLa cells is intercellular adhesion molecule 1. Proc. Natl. Acad. Sci. USA **86:**4907–4911.
31. **Uncapher, C. R., C. M. Dewitt, and R. J. Colonno.** 1991. The major and minor group receptor families contain all but one human rhinovirus serotype. Virology **180:**814–817.
32. **vanDriel, I. R., J. L. Goldstein, T. C. Sudhof, and M. S. Brown.** 1987. First cysteine-rich repeat in ligand-binding domain of low density lipoprotein receptor binds Ca2+ and monoclonal antibodies, but not lipoproteins. J. Biol. Chem. **262:**17443–17449.
33. **Verdaguer, N., I. Fita, M. Reithmayer, R. Moser, and D. Blaas.** 2004. X-ray structure of a minor group human rhinovirus bound to a fragment of its cellular receptor protein. Nat. Struct. Mol. Biol. **11:**429–434.
34. **Vlasak, M., S. Blomqvist, T. Hovi, E. Hewat, and D. Blaas.** 2003. Sequence and structure of human rhinoviruses reveal the basis of receptor discrimination. J. Virol. **77:**6923–6930.
35. **Willnow, T. E., and J. Herz.** 1994. Genetic deficiency in low density lipoprotein receptor-related protein confers cellular resistance to Pseudomonas exotoxin A. Evidence that this protein is required for uptake and degradation of multiple ligands. J. Cell Sci. **107:**719–726.
36. **Yamamoto, T., C. G. Davis, M. S. Brown, W. J. Schneider, M. L. Casey, J. L. Goldstein, and D. W. Russell.** 1984. The human LDL receptor: a cysteine-rich protein with multiple Alu sequences in its mRNA. Cell **39:**27–38.
37. **Yin, F. H., and N. B. Lomax.** 1983. Host range mutants of human rhinovirus in which nonstructural proteins are altered. J. Virol. **48:**410–418.